Research Square

Preprints are preliminary reports that have not undergone peer review.
They should not be considered conclusive, used to inform clinical practice,
or referenced by the media as validated information.

Silymarin extract outperforms its nanomodified form in inhibiting colon cancer cell proliferation

Naglaa Fatahy
University of Sadat City
Khalid Bassiouny
University of Sadat City
Mahmoud Al-Saman
University of Sadat City
Aysam M. Fayed
University of Sadat City
Ahmed M. Tabl
University of Sadat City
Amal A. Abd-El-Aziz
University of Sadat City
Hany Khalil
hany.khalil@gebri.usc.edu.eg
University of Sadat City

Research Article

Keywords: Colon cancer, Silymarin, Nano-Silymarin, Raf-1 signaling, P53

Posted Date: July 3rd, 2026

DOI: https://doi.org/10.21203/rs.3.rs-9596311/v1

License: This work is licensed under a Creative Commons Attribution 4.0 International License.
Read Full License

Additional Declarations: No competing interests reported.

Silymarin extract outperforms its nanomodified form in inhibiting colon cancer cell proliferation

Naglaa Fatahy[1], Mai A. Daha[1], Khalid Bassiouny[1], Mahmoud Al-Saman[2], Aysam M. Fayed[1], Ahmed M. Tabl[1], Amal A. Abd-El-Aziz[1], and Hany Khalil[1,3]*

[1]Department of Molecular Biology, Faculty of Biotechnology, University of Sadat City, Sadat City, Egypt.

[2]Industrial Biotechnology Department, Faculty of Biotechnology, University of Sadat City, Sadat City, Egypt.

[3]Center for Converging Sciences and Emerging Technologies (CoSET), Benha National University (BNU), El-Obour City, P.O. 13518, Egypt.

*Corresponding author:

Prof. Dr. Hany Khalil

Department of Molecular Biology,

Faculty of Biotechnology

University of Sadat City, 32879 Sadat City, Egypt

Tel : + 2048- 2601265/2601267

Fax :+ 2048 – 2601266/2601268

E-mail: hany.khalil@gebri.usc.edu.eg, hany.mohamed@bnu.edu.eg

Abstract

Colon cancer, including rectal tumors, remains a prevalent global malignancy with rising cases among younger people and transitioning regions. Silymarin, a plant-based extract with antioxidant, anti-inflammatory, and anticancer effects, is increasingly studied for its potential therapeutic value, clinical applications worldwide. In this study, we aimed to develop a nanostructured formulation of Silymarin, evaluate its anticancer efficacy compared with the native extract, assess its cytotoxicity, and investigate the underlying molecular mechanisms in colon cancer cells. Nano-Silymarin was prepared by dissolving the silymarin extract in an oil phase containing the emulsifier Span 80, followed by high-pressure homogenization to produce droplets under 100 nm in diameter. The antiproliferative effects of Nano-Silymarin were tested in Caco-2 colon cancer cells and compared with those of the original silymarin extract in both Caco-2 cells and NCM-460 normal colon epithelial cells. Our results showed that the normal Silymarin extract reduced Caco-2 cell viability at lower concentrations than Nano-Silymarin, while sparing normal epithelial cells. In contrast, Nano-Silymarin significantly decreased the viability of NCM-460 cells at equivalent doses. At 1.25mg/mL, the original extract markedly reduced viable cancer cell numbers, induced apoptosis in nearly 50% of Caco-2 cells and preserved the viability of normal cells. qRT-PCR analysis revealed that treatment with original Silymarin downregulated Raf-1 and ERK, key regulators in the MAPK proliferation pathway, while upregulating the tumor suppressor P53 and apoptotic mediator caspase-3. ELISA assays further showed that, unlike Nano-Silymarin, the original extract produced a time-dependent decrease in TNF-α, increased IL-6, and progressively elevated the levels of anti-inflammatory cytokines IL-4 and IL-10. In summary, when comparing the Silymarin extract to its nanostructured counterpart, the original form demonstrated superior anticancer activity through inhibition of proliferation pathways and activation of P53-mediated apoptosis, with minimal toxicity toward normal colon epithelial cells.

Keywords: Colon cancer, Silymarin, Nano-Silymarin, Raf-1 signaling, P53

Introduction

Colon cancer, referred to as colorectal cancer when it includes the rectum, is a malignancy that develops in the large intestine, the final section of the digestive tract. It typically begins as small, noncancerous growths called polyps on the inner lining of the colon [1]. The disease progresses through a multistep process over several years, during which healthy colon cells gradually transform into malignant ones through a series of genetic and cellular changes [2]. Early development often involves mutations in key genes, such as *KRAS,* an oncogene that drives uncontrolled cell proliferation, and *TP53*, a tumor suppressor whose loss of function allows cells to bypass programmed cell death [3]. As the condition advances, adenomatous polyps (adenomas) emerge in the colon lining. Treatment decisions depend on cancer stage, patient health, and tumor-specific features. Standard chemotherapy protocols, such as FOLFOX (5-fluorouracil, leucovorin, oxaliplatin) and CAPOX (capecitabine, oxaliplatin), are widely used [4]. However, their limited effectiveness and significant toxicity, as reported in multiple studies, highlight the urgent need for new, more effective therapeutic agents against colon cancer [5].

Silymarin extract is a mixture of flavonolignans derived from the seeds of *Silybum marianum*. Its principal active component is silybin (silybin), accompanied by isosilybin, silydianin, and silychristin [6]. Traditionally and in modern medicine, silymarin has been used for various conditions due to its antioxidant, anti-inflammatory, antifibrotic, and membrane-stabilizing properties. In chronic liver diseases such as alcoholic liver disease and hepatitis B and C virus infections, silymarin has been reported to scavenge free radicals, thereby reducing oxidative stress in hepatocytes [7,8]. It also acts as a membrane stabilizer for hepatocytes by decreasing toxin penetration and inhibiting lipid peroxidation. This helps slow fibrosis progression through modulation of liver enzyme levels (ALT, AST). However, evidence regarding its impact on survival in severe liver disease remains mixed. Clinically, silymarin extract is used as an adjunct therapy in *Amanita phalloides* (death cap mushroom) poisoning, where intravenous silibinin is sometimes administered to block toxin uptake [9]. In cancer research, animal studies have shown that silymarin exerts anti-proliferative and pro-apoptotic effects on certain cancer

cells [10]. Furthermore, it has demonstrated chemoprotective potential by reducing chemotherapy-induced liver and kidney toxicity.

Nanotechnology has emerged as a transformative tool in both cancer treatment and diagnostics, with significant promise in oncotherapy [11]. Despite decades of research, cancer remains a leading global health threat. Chemotherapy remains the most widely used cancer treatment, yet its efficacy is often compromised by severe toxicity and adverse effects [12]. A major challenge is the lack of efficient delivery systems for hydrophobic anticancer drugs, whose low solubility in aqueous media limits intravenous administration [13]. To overcome these limitations, researchers are exploring alternative, cost-effective strategies capable of addressing the drawbacks of conventional chemotherapy. Among these, cancer nanotechnology is gaining attention for its potential in targeted drug delivery, molecular diagnostics, and imaging. Nanodrug delivery systems can enhance the cellular targeting of anticancer agents and improve radio-sensitization. Consequently, the development of nanocarrier systems for anticancer drugs is a key focus for improving drug solubility and therapeutic efficacy [14]. However, they also present potential drawbacks and toxicities. For instance, nanoparticles can exhibit unexpected behavior in the body, altering their absorption, distribution, metabolism, and excretion. Importantly, they may induce the generation of reactive oxygen species (ROS), which can damage lipids, proteins, and DNA, disrupt cellular energy metabolism, and physically compromise lipid bilayer integrity [15].

Building on these properties, the present study aims to compare and evaluate the antiproliferative effects of silymarin extract and its nanostructured formulation in colon cancer cells *in vitro*.

Material and Methods

Preparation of agent

Fruits of *Silybum marianum* (milk thistle) were collected from a private farm in Mansoura City, northern Egypt (30.9416° N, 31.2904° E). The fruits were surface sterilized with 75% ethanol, thoroughly rinsed with distilled water, and air-dried under sterile conditions. Subsequently, the dried fruits were ground in a sterilized mortar and pestle under liquid nitrogen until a homogeneous powder was obtained. The silymarin extract was dissolved in dimethyl sulfoxide (DMSO) to prepare a stock solution by dissolving 30 mg of extract in 1 mL of DMSO. Serial dilutions were then prepared to obtain final concentrations of 10, 5, 2.5, and 1.25 µg/mL. The prepared solutions were transferred into sterile tubes and stored at 4°C until further use.

Silymarin-loaded nanospanlastics preparing protocol

To prepare the oil phase, 50 µg of Silymarin was dissolved in 10 mL of omega-9 fatty acid (oleic acid). Following this, 160 mg of sorbitan monooleate (Span 80) was added and dissolved in a 1:1 mixture of chloroform and ethanol using a round-bottom flask. The organic solvents were then removed under vacuum using a rotary evaporator (Rotavapor, Heidolph VV 2000, Burladingen, Germany) set at 100 rpm [16], forming a thin lipid film on the flask wall. This film was subsequently hydrated with 10 mL of phosphate-buffered saline (PBS, pH 7.4) containing 40 mg of Tween 80, which acted as the edge activator (EA). To reduce the size of the resulting vesicles, the suspension was subjected to bath sonication for five minutes. The morphology and particle size of Silymarin was characterized using an automated microscope imaging system. Samples were appropriately diluted with deionized water, mounted on clean glass slides, and imaged under standardized magnification and illumination settings. Automated image-analysis software was employed to identify individual particles and determine their diameters, from which particle-size distributions and mean particle sizes were calculated. Surface charge and colloidal stability were evaluated by measuring zeta potential using a zeta-potential analyzer based on electrophoretic light scattering (ELS). Diluted samples were transferred into disposable zeta cells, and measurements were performed at room

temperature. Electrophoretic mobility values were converted to zeta potential using the Smoluchowski model. To assess colloidal stability, Silymarin suspension was initially monitored for 6 min to confirm immediate dispersion stability and subsequently evaluated over 24 h. Particle size and polydispersity index (PDI) were measured at predetermined intervals using dynamic light scattering (DLS). All measurements were conducted in triplicate and reported as mean ± standard deviation.

Cell lines

Normal human colonic epithelial cells (NCM460) and human colorectal adenocarcinoma cells (Caco-2) were obtained from VacSera (Doki, Egypt). Both cell lines were cultured in RPMI-1640 medium supplemented with 10% heat-inactivated fetal bovine serum, 4 mM sodium pyruvate, and 4 mM L-glutamine. Cells were maintained at 37°C under a humidified atmosphere containing 5% CO_2. Cell morphology was monitored and documented using a Zeiss A-Plan inverted microscope equipped with a 10× objective lens.

Cell viability and cytotoxic concentration 50% (CC_{50})

The cytotoxic potential of Silymarin and Nano-Silymarin was investigated in both NCM-460 and Caco-2 cell lines. Cells were plated in 96-well culture plates at a density of 1×10^4 cells per well and allowed to adhere under standard incubation conditions (37°C, 5% CO_2). Following attachment, cells were exposed to increasing concentrations of each test compound ranging from 0 to 10 mg/mL and incubated for 24 h. Cellular viability was subsequently determined using the MTT colorimetric assay according to the manufacturer's protocol. The reduction of MTT to insoluble formazan crystals by metabolically active cells was quantified spectrophotometrically at 570 nm. Viability percentages were calculated relative to untreated controls, and the half-maximal cytotoxic concentration (CC_{50}) was estimated as the concentration required to decrease cell viability by 50% [17].

Proliferation assay

Changes in cellular morphology and the number of viable cells were evaluated in both Caco-2 and NCM-460 cultures following treatment. For confirmation of microscopic observations, duplicate cultures were established in 6-well plates at a seeding density of 1 × 10^5 cells per well. After attachment, cells were exposed to either Silymarin or Nano-Silymarin at a concentration of 1.25 mg/mL and maintained under standard culture conditions for 24 h. At the end of the treatment period, morphological alterations were documented using an inverted light microscope. To quantify cell survival, the culture medium was carefully discarded, and adherent cells were detached by treatment with trypsin for 3 min at 37°C. The harvested cells were subsequently washed twice with phosphate-buffered saline (PBS) and resuspended in complete RPMI-1640 medium. Cell enumeration was performed using a hemocytometer. Briefly, 10 µL of the resulting cell suspension was transferred to the counting chamber, and viable cells were counted microscopically. The final concentration of living cells was expressed as cells/mL and calculated by multiplying the average cell count by a factor of 100 [18,19].

Lactate dehydrogenase (LDH) production

Cell membrane integrity and cytotoxicity were evaluated by measuring the release of lactate dehydrogenase (LDH) into the culture medium using a commercial LDH Assay Kit (Abc-65393). LDH is a stable cytosolic enzyme that is released into the extracellular environment upon damage to the plasma membrane; therefore, its activity serves as an indicator of cellular injury and cell death. Following the experimental treatments, cell lysates were prepared according to the manufacturer's protocol. Briefly, 100 µL of each lysate sample was transferred into the wells of a microplate and mixed with an equal volume (100 µL) of the prepared LDH reaction reagent. The reaction mixtures were incubated at room temperature for 30 min under protected light conditions to allow enzymatic conversion of the substrate into a detectable colored product. After completion of the reaction, the absorbance was measured at 450 nm using a microplate reader. The intensity of the color produced was directly proportional to the amount of LDH activity present in the sample. All measurements were performed according to the instructions

provided by the manufacturer. The obtained optical density (OD) values were recorded and averaged for each experimental group. To facilitate comparison among treatment groups, the mean absorbance values of treated samples were normalized against the corresponding untreated control group. The normalized data were subsequently expressed as fold changes relative to the control, which was assigned a value of 1. An increase in fold change indicated enhanced LDH release and, consequently, greater cellular membrane damage and cytotoxicity.

Annexin-V assay

The apoptotic response of Caco-2 cells following treatment with Silymarin and Nano-Silymarin was investigated using Annexin V-FITC/Propidium Iodide (PI) dual staining coupled with flow cytometric analysis. This assay enables discrimination between viable cells, early apoptotic cells, late apoptotic cells, and necrotic cells based on phosphatidylserine externalization and plasma membrane integrity. The procedure was carried out using a commercially available Annexin V-FITC/PI Apoptosis Detection Kit (BD Biosciences) in accordance with the manufacturer's recommendations. Briefly, Caco-2 cells were seeded into sterile 25 cm^2 tissue culture flasks at a density of 1×10^4 cells per flask and maintained overnight under standard culture conditions (37°C in a humidified atmosphere containing 5% CO_2) to allow cell attachment and stabilization. Following incubation, the culture medium was replaced with fresh medium containing either Silymarin or Nano-Silymarin at a final concentration of 1.25 mg/mL. Cells were then incubated for an additional 24 h to evaluate the apoptotic effects of the treatments. At the end of the exposure period, both adherent and floating cells were collected to ensure accurate assessment of all cell populations. The harvested cells were washed twice with cold PBS to remove residual medium and treatment compounds. Subsequently, the cell pellet was gently resuspended in Annexin V Binding Buffer to obtain a homogeneous single-cell suspension suitable for staining. For apoptosis detection, 100 µL of the prepared cell suspension was transferred to a flow cytometry tube and incubated with 20 µL of Annexin V-FITC and 10 µL of PI. The samples were protected from light and incubated at room temperature for 30 min to allow adequate binding of the fluorescent

probes. Following staining, 500 µL of Binding Buffer was added to each tube to facilitate flow cytometric acquisition. The stained samples were analyzed within 1 h using a flow cytometer. Data were collected and interpreted based on fluorescence intensity profiles. Cells negative for both Annexin V and PI were classified as viable cells, Annexin V-positive/PI-negative cells were considered early apoptotic, Annexin V-positive/PI-positive cells were identified as late apoptotic, whereas Annexin V-negative/PI-positive cells were categorized as necrotic. The percentages of cells in each population were calculated and compared among the experimental groups to determine the pro-apoptotic effects of Silymarin and Nano-Silymarin treatments [17,20].

Quantitative real-time PCR

The impact of Silymarin and Nano-Silymarin on the transcriptional expression of selected genes associated with cell proliferation, signal transduction, and apoptosis was evaluated using quantitative real-time polymerase chain reaction (qRT-PCR). For this purpose, cells were cultured in duplicate in 6-well plates at a density of 1×10^5 cells per well and allowed to attach under standard growth conditions. After stabilization, the cultures were exposed to either Silymarin or Nano-Silymarin at a concentration of 1.25 mg/mL and incubated for 24 h. Following treatment, total cellular RNA was isolated using TRIzol® reagent (Invitrogen, USA) according to the manufacturer's instructions. The extracted RNA was subsequently purified using a commercial RNA purification system to improve RNA quality and remove potential contaminants. RNA concentration and purity were assessed prior to downstream applications. For first-strand complementary DNA (cDNA) synthesis, 1 µg of purified total RNA was reverse-transcribed using Moloney Murine Leukemia Virus (M-MLV) reverse transcriptase (Promega, USA). Quantitative analysis of gene expression was performed using the QuantiTect SYBR Green PCR Kit (Qiagen, USA) and gene-specific primers (Table 1). The transcriptional levels of Raf-1, ERK, p53, and caspase-3 (CAS3) were investigated as molecular markers associated with cell survival, signaling pathways, and programmed cell death. Glyceraldehyde-3-phosphate dehydrogenase (GAPDH) was employed as the housekeeping gene to normalize variations in RNA input and amplification efficiency

among samples. Each qRT-PCR reaction mixture was prepared in a final volume containing 10 µL of SYBR Green master mix, 0.2 µM of forward and reverse primers, 0.25 µL RNase inhibitor, nuclease-free water, and 2 µL of synthesized cDNA template. Amplification reactions were carried out under the following thermal cycling conditions: an initial denaturation step at 94°C for 5 min to activate the reaction and denature double-stranded DNA, followed by 35 amplification cycles consisting of denaturation at 94°C for 30 s, primer annealing at 60°C for 15 s, and extension at 72°C for 30 s. Fluorescence signals generated during amplification were continuously monitored, and threshold cycle (Ct) values were recorded for each sample. Relative mRNA expression levels were calculated after normalization to GAPDH expression and were subsequently compared among experimental groups to determine the regulatory effects of Silymarin and Nano-Silymarin on the target genes [21,22].

Table 1: Oligonucleotides sequences used for mRNA quantification of indicated genes

Description	Primer sequences 5'-3'
Raf-1 sense	TTTCCTGGATCATGTTCCCCT
Raf-1 antisense	ACTTTGGTGCTACAGTGCTCA
ERK sense	ACAGGCTGTTCCCAAATGCT
ERK antisense	CGAACTTGAATGGTGCTTCG
P53 sense	AGAGTCGGATTCGCCGCCGCA
P53 antisense	GACGGCATGGTGCAGGGATCT
CAS3 sense	CAGTGGAGGCCGACTTC TTG
CAS3 antisense	TGGCACAAAGCGACTGGAT
GAPDH-sense	AACATCAGACCTACTGCCAGCGC
GAPDH-antisense	CGCAGGATCTGGTAGAGGAAGT

Enzyme-linked immunosorbent assay (ELISA)

The effects of Silymarin and Nano-Silymarin on the production of inflammatory and anti-inflammatory cytokines by Caco-2 cells were evaluated using enzyme-linked immunosorbent assay (ELISA). The concentrations of interleukin-4 (IL-4), IL-6, IL-10, and tumor necrosis factor-alpha (TNF-α) were determined using commercially available

human ELISA kits (Abcam, UK), including ab46058 for IL-4, ab46027 for IL-6, ab46034 for IL-10, and ab100654 for TNF-α. These cytokines were selected to assess the immunomodulatory and inflammatory responses induced by the tested formulations. Briefly, Caco-2 cells were seeded into 96-well culture plates and maintained under standard cell culture conditions until reaching the appropriate level of attachment and growth. The cells were subsequently exposed to either Silymarin or Nano-Silymarin at a concentration of 1.25 µg/mL. Following treatment, the cultures were incubated for different exposure periods (0, 6, 12, 24, 48, and 72 h) to investigate the time-dependent effects of both formulations on cytokine production. At each designated time point, cellular proteins were extracted by adding 100 µL of cell lysis buffer (Invitrogen, USA) to each well. The plates were gently agitated to ensure complete cell disruption and uniform sample preparation. The resulting lysates were carefully collected and transferred to ELISA wells pre-coated with capture antibodies specific for each cytokine. For cytokine quantification, 50 µL of the appropriate standard or control solution and 50 µL of 1× biotin-conjugated detection antibody were added to each well containing the samples. The plates were then incubated for 2 h at room temperature to facilitate antigen-antibody binding. Following incubation, the wells were washed according to the manufacturer's protocol to remove unbound components. Subsequently, 100 µL of 1× streptavidin-horseradish peroxidase (HRP) conjugate was added to each well, and the plates were incubated for 30 min in the dark at room temperature. After an additional washing step, 100 µL of tetramethylbenzidine (TMB) substrate solution was added. The enzymatic reaction was allowed to proceed for 15 min under light-protected conditions, resulting in the development of a blue color proportional to the concentration of the target cytokine present in the sample. The reaction was terminated by adding 100 µL of stop solution to each well, causing a color change from blue to yellow. Absorbance was immediately measured at 450 nm using a microplate spectrophotometer. Cytokine concentrations were calculated from standard calibration curves generated for each assay and expressed relative to the corresponding control group. The obtained data were subsequently used to compare the influence of Silymarin and Nano-Silymarin on inflammatory signaling and cytokine secretion profiles in Caco-2 cells over time [21,23].

Data analysis

All experimental data were compiled, organized, and processed using Microsoft Excel software. The program was utilized for data management, calculation of descriptive statistics, graphical representation of results, and generation of figures and charts. Quantitative results obtained from the various biological assays were expressed as mean values derived from replicate experiments. Statistical comparisons between experimental and control groups were performed using a two-tailed Student's T-test to determine whether observed differences were statistically significant. This test was selected to evaluate differences in measured parameters between two independent groups while considering variation in both directions. Statistical significance was accepted at a probability level (p) of less than 0.05, indicating that the likelihood of obtaining the observed differences by chance was less than 5%. Relative gene expression data generated by qRT-PCR were analyzed using the comparative threshold cycle (Ct) method, commonly referred to as the 2^–ΔΔCt method. This approach enables the determination of fold changes in target gene expression relative to a reference sample after normalization to an endogenous control gene. For each sample, the threshold cycle (Ct) value of the housekeeping gene GAPDH was subtracted from the Ct value of the target gene to correct for differences in RNA quantity and reverse transcription efficiency: ΔCt = Ct (target gene) − Ct (GAPDH). The normalized Ct value obtained from the control group was used as a calibrator. The ΔΔCt value for each treated sample was calculated by subtracting the mean ΔCt of the control group from the ΔCt of the corresponding experimental group: ΔΔCt = ΔCt (treated sample) − ΔCt (control sample). Changes in mRNA expression were expressed as fold differences relative to the control group using the following equation: Relative Expression (Fold Change) = 2^−ΔΔCt. A fold-change value greater than 1 indicated upregulation of gene expression, whereas a value less than 1 reflected downregulation relative to the untreated control. The resulting data were subsequently subjected to statistical evaluation, and differences were considered significant when the calculated p-value was below 0.05 [2,24].

Results

Nanomodification oncome of Silymarin to a Nano-Silymarin form

To assess the purity and confirm the nanomodified form of Silymarin, UV-Visible absorption spectroscopy was used to compare two samples: the crude water extract (CWE, red curve) and Silymarin-loaded nanoparticles (CWE-NPs, black curve). Both spectra exhibit characteristic peaks of flavonolignans and phenolic compounds. The peak at 247 nm corresponds to $\pi \rightarrow \pi^*$ transitions in aromatic rings, while the 285 nm peak is attributed to $n \rightarrow \pi^*$ transitions associated with carbonyl groups (C=O), indicative of compounds like silibinin. In Figure 1A, a red shift observed in CWE-NPs suggests changes in the electronic environment due to encapsulation or interaction with nanoparticles, possibly through hydrogen bonding or van der Waals forces. CWE-NPs also showed higher absorbance at key wavelengths, particularly at 285 nm, implying improved solubility or stability of active components in the nanomodified form. Additionally, the broader spectrum of CWE-NPs indicates reduced particle size, increased surface area, and potential nanoparticle aggregation. Figure 1B further confirms nanomodification, where increased absorbance in the UV range reflects enhanced solubility or dispersion of Nano-Silymarin. The absence of new peaks in the visible region suggests the use of non-metallic nanocarriers such as polymers or liposomes. Transmission Electron Microscopy (TEM) provided visual confirmation of nanostructure. As shown in Figure 3C, nanoparticles appear as dark, nearly spherical or irregular regions within a lighter background, likely representing a carrier matrix. Measurements (0.20 μm to 0.51 μm) confirm the particles fall within the nano-to-submicron range, suitable for drug delivery applications due to their favorable morphology and dispersity. Figure 1D shows size distribution by intensity, revealing a polydisperse sample with multiple peaks. The dominant peak around ~500 nm indicates a significant population of particles in this size range, possibly due to agglomeration or incomplete processing. While this still aligns with the nanoparticle domain, it suggests the need for optimization in the formulation process to reduce heterogeneity and improve stability.

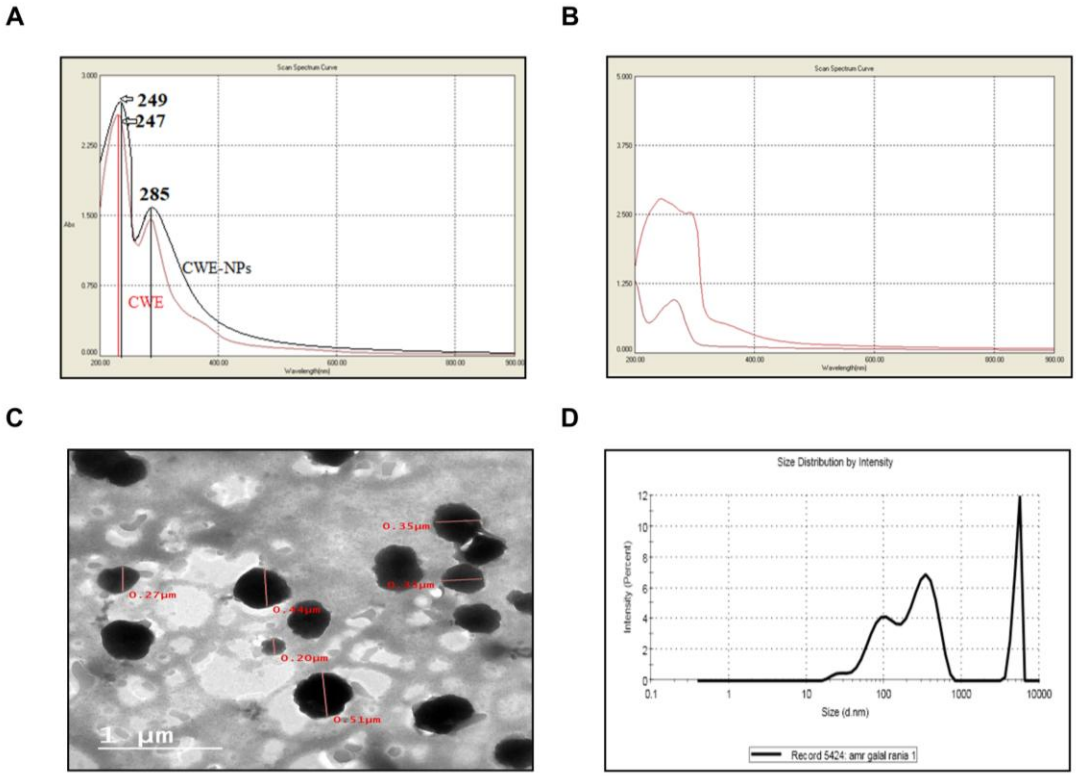


Figure 1: Comparative analysis of electrical potential and structural changes between Nano-Silymarin and non-modified Silymarin.

(A) UV-Vis absorbance spectra: The red curve (CWE – Crude Extract) shows peaks at 247 nm and 285 nm, while the black curve (CWE-NPs – Nano-Silymarin) exhibits a slightly red-shifted peak at 249 nm and a more pronounced peak at 285 nm, indicating possible structural modifications during nanoparticle formation. (B) The UV-Vis spectrum plot displays absorbance (Y-axis) versus wavelength (X-axis, 200–900 nm), used to assess molecular structural changes associated with nanoparticle synthesis or modification. (C) TEM (Transmission Electron Microscopy) image: Visualizes the nanoparticles at micro- and nano-scales, with particle sizes ranging from 0.20 µm to 0.51 µm, as indicated by red markers and a scale bar of 1 µm. (D) Dynamic Light Scattering (DLS) analysis: Shows particle size distribution by intensity. The X-axis represents particle diameter (nm), while the Y-axis reflects the relative light intensity scattered, providing insight into the size distribution of Nano-Silymarin particles.

Silymarin demonstrates stronger antiproliferative effects than its nanomodified form in Caco-2 cells

The potential antiproliferative activities of Silymarin and Nano-Silymarin were assessed in the Caco-2 colorectal cancer cell line and compared with their effects on normal colon cells (NCM-460). Both cell types were seeded in 96-well plates and treated with varying concentrations of the compounds (0.6–10 mg/mL) for 24 hours, with DMSO serving as the control. As shown in Figure 2A, Silymarin significantly reduced Caco-2 cell viability in a dose-dependent manner, based on MTT assay absorbance measurements. In contrast, Nano-Silymarin produced negligible changes in Caco-2 viability compared to the control. Importantly, both Silymarin and Nano-Silymarin exhibited no detectable toxicity toward NCM-460 cells, maintaining viability levels comparable to those of DMSO-treated and untreated controls (Figure 2B). Overall, these findings indicate that the original form of Silymarin exerts a pronounced antiproliferative effect on Caco-2 cells across the tested concentration range, while sparing normal colon cells, similar to Nano-Silymarin, which showed minimal impact on cancer cell proliferation.

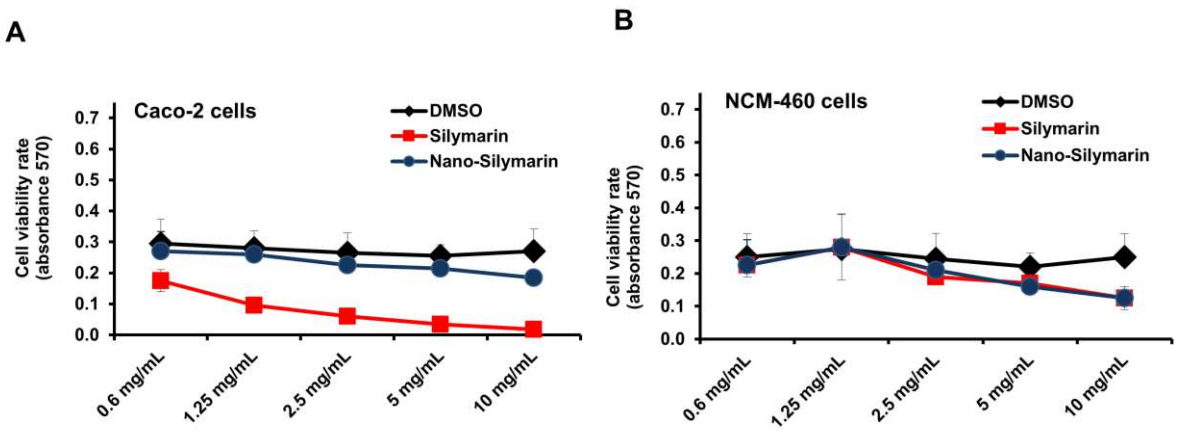


Figure 2: Evaluation of cell viability and cytotoxic effects of Silymarin and Nano-Silymarin in colon cancer and normal colon cell lines.

(A) Cell viability of Caco-2 colon cancer cells was measured after 24-hour exposure to various concentrations of Silymarin and Nano- Silymarin, with DMSO-treated cells serving as the control. (B) Viability of normal colon epithelial cells was assessed following treatment with the same concentration range of Silymarin and Nano-Silymarin, compared to DMSO controls. Error bars indicate standard deviation (SD) from three replicates, and the results are representative of three independent experiments.

Cytotoxic effects and morphological changes in colon cancer cells following treatment with Silymarin and Nano-Silymarin

The effects of Silymarin and Nano-Silymarin on cell viability and morphology were evaluated in both normal and cancerous colon cells. As shown in Figure 3A, NCM-460 normal colon cells exhibited noticeable morphological alterations after treatment with 1.25 mg/mL Nano-Silymarin, whereas cells exposed to the same concentration of the original Silymarin maintained a morphology similar to that of the untreated controls. In Caco-2 colon cancer cells, marked morphological changes were observed only in response to the original Silymarin. Treatment with 1.25 mg/mL of this formulation significantly reduced the number of viable cancer cells compared to the control, while Nano-Silymarin had no significant effect on cancer cell viability. Both formulations showed negligible impact on normal cell counts (Figure 3B). LDH release, used as an indicator of cellular damage, was significantly increased, by approximately fivefold, in Caco-2 cells treated with 1.25 mg/mL of original Silymarin compared with control, DMSO-treated, and Nano-Silymarin-treated cells. In contrast, the positive control Triton X-100 induced a ninefold LDH increase (Figure 3C). Overall, these results indicate that the original form of Silymarin exerts stronger antiproliferative and cytotoxic effects on colon cancer cells than its nano-formulation, while maintaining minimal toxicity toward normal colon cells.

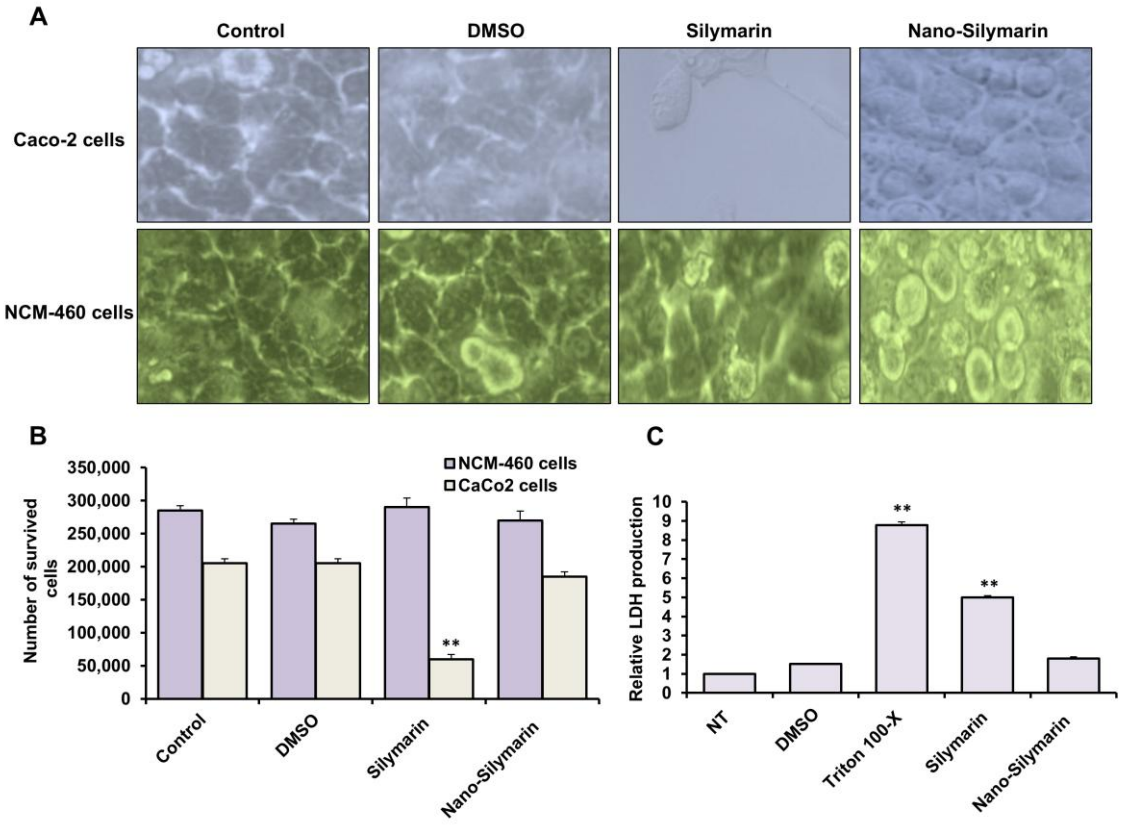


Figure 3: Impact of Silymarin and Nano-Silymarin on cell morphology and viability.

(A) Morphological alterations in Caco-2 and NCM-460 cells were examined 24 hours after exposure to 1.25 mg/mL Silymarin or Nano-Silymarin using an inverted microscope. Untreated cells (Control) and DMSO-treated cells served as controls. (B) Cell survival was quantified after 24 hours of treatment with 1.25 mg/mL of the indicated compounds. (C) Cytotoxicity in Caco-2 cells was evaluated by measuring relative LDH release following treatment with each Silymarin formulation. Triton X-100–treated cells were used as the positive control for cytotoxicity. Data represent the mean ± SD from three independent experiments. Statistical significance was determined by two-tailed Student's *t*-test; $P \leq 0.05$, $P \leq 0.01$.

Silymarin exhibits significant effects overall apoptotic signaling on Caco-2 cells

To assess the effects of Silymarin extract and its nano-formulation on programmed cell death (PCD) and apoptotic signaling in Caco-2 cells treated with 1.25 mg/mL, we performed Annexin V assays using flow cytometry. These assays measured early and late apoptosis, as well as overall cell death. As shown in Figures 4A and 4B, Silymarin extract had a marked effect on PCD, as evidenced by Annexin V staining. Cells treated with the DMSO control exhibited minimal apoptotic activity and low levels of cell death, confirming that the solvent did not significantly influence PCD. In contrast, treatment with Silymarin extract led to a substantial increase in apoptotic activity, with nearly 40% of cells undergoing late apoptosis after 24 hours. By comparison, the nano-form of Silymarin at the same concentration induced late apoptosis in less than 10% of cells. Notably, both forms of Silymarin showed minimal impact on overall cell death after 24 hours, suggesting that while the extract strongly initiates apoptotic signaling, the full progression of PCD may occur beyond the 24-hour mark. These findings underscore the potent pro-apoptotic activity of the Silymarin extract and indicate that it is significantly more effective than the nano-form in inducing apoptosis in Caco-2 cells.

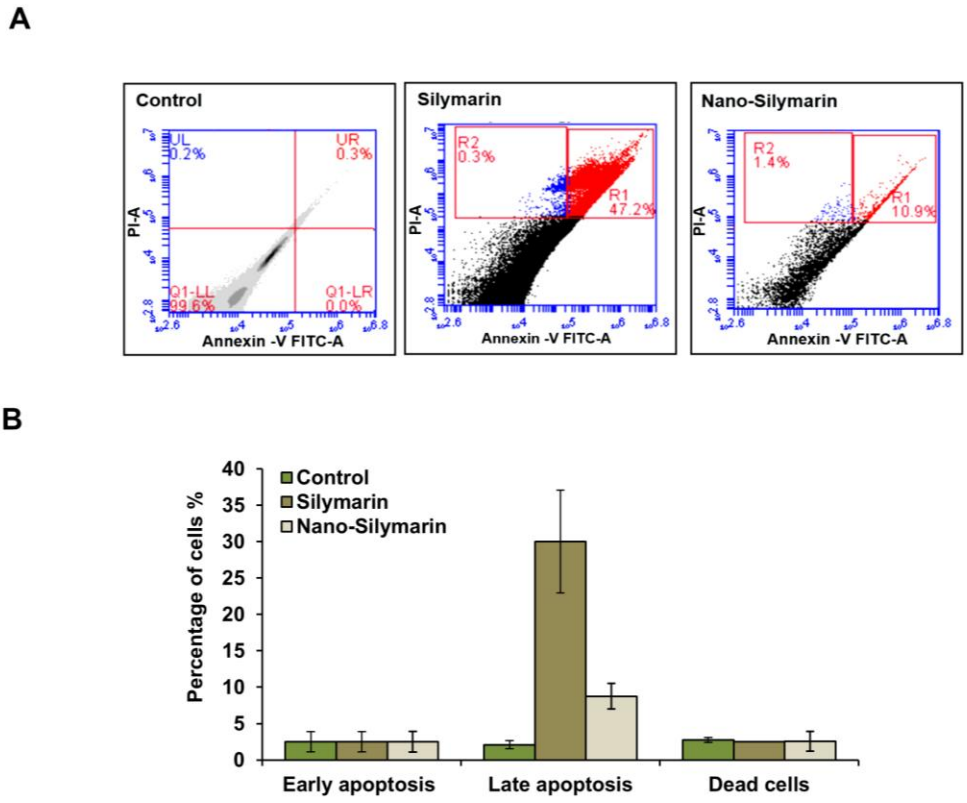


Figure 4: The apoptotic response to drug treatment in colon cancer cells

(A) Caco-2 cells were exposed to 1.25 mg/mL µM of each specified Silymarin forms for 24 hours, followed by staining with Annexin V+/Propidium Iodide (PI). Early and late apoptotic signaling, as well as dead cells, were analyzed via flow cytometry. (B) The flow cytometry results were used to determine the percentage of cells exhibiting early or late apoptosis and those that were dead. The data represent the mean ± SD from three independent experiments. Statistical significance was assessed using a two-tailed Student's t-test, with (*) indicating P-values ≤ 0.05 and (**) indicating P ≤ 0.01.

Silymarin suppresses the expression of Raf-1 and ERK gene expression and enhances P53 and CAS3 expression in Caco-2 cells

The potential antiproliferative effect of Silymarin warrants further investigation due to its impact on cell proliferation and associated signaling pathways in cancer cells. Among the key genes involved in proliferative signaling are Raf-1 and the transcription factor ERK. Additionally, the tumor suppressor gene P53 is known to be upregulated in response to disturbances in the Raf-1/ERK signaling pathway. To determine whether the original form of Silymarin and its nanomodified form influence the expression of these genes and affect cancer cell proliferation and cell death, the expression levels of Raf-1, ERK, P53, and CAS3 were assessed in Caco-2 cells treated with 1.25 mg/mL of either Silymarin or Nano-Silymarin for 24 hours. As shown in Figure 5A, qRT-PCR analysis revealed a significant downregulation of Raf-1 expression in Silymarin-treated cells compared to non-treated (NT) and DMSO-treated controls, while Nano-Silymarin treatment had negligible effects. Similarly, the expression of ERK was significantly reduced in cells treated with the original Silymarin extract compared to all control groups, including Nano-Silymarin-treated cells (Figure 5B). Furthermore, P53 expression was significantly upregulated, by approximately 3.5-fold, in Silymarin-treated cells compared to control and Nano-Silymarin-treated groups (Figure 5C). In line with this, a significant increase in CAS3 gene expression (approximately 2.5-fold) was also observed following treatment with the original form of Silymarin (Figure 5D). Collectively, these findings suggest that the original Silymarin extract more effectively suppresses proliferation-related gene expression and enhances the expression of pro-apoptotic genes P53 and CAS3 in Caco-2 cells compared to its nanomodified counterpart.

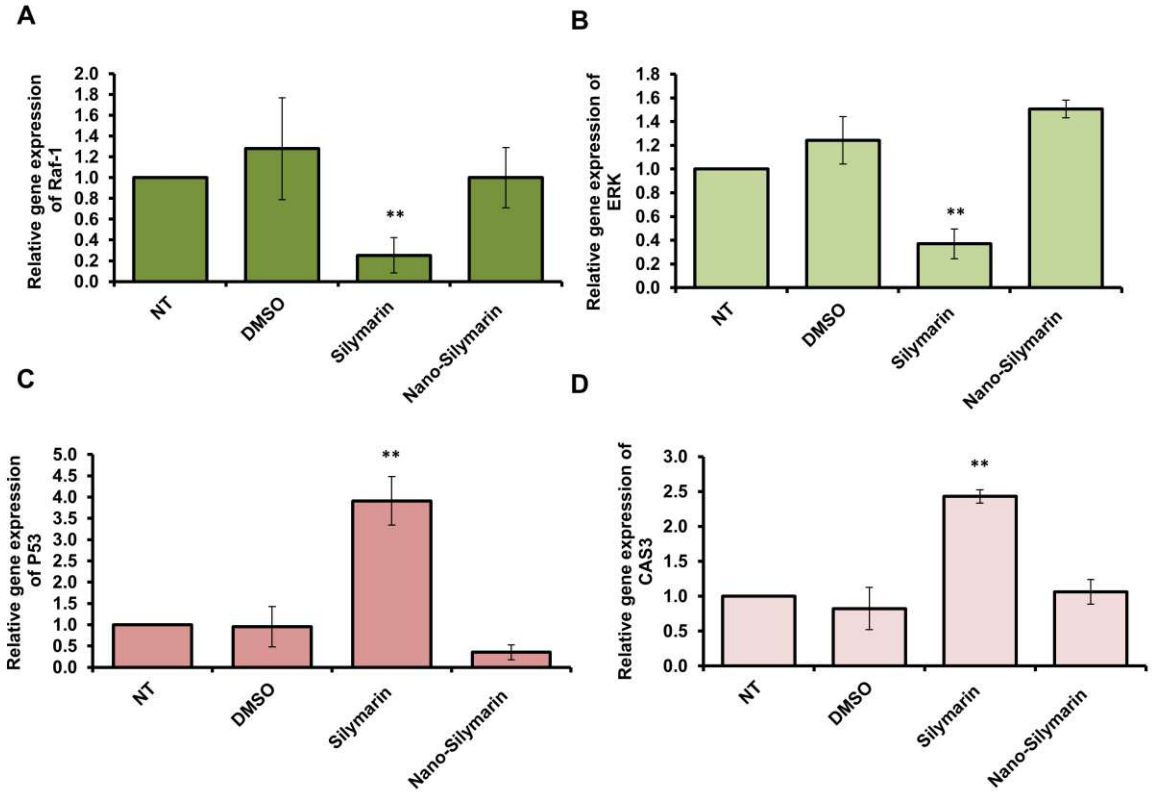


Figure 5: Analysis of Raf-1/ERK, and P53/CAS in Silymarin and Nano-Silymarin–treated Caco-2 cells.

(A) The relative mRNA expression of Raf-1 was measured in Caco-2 cells treated with 1.25 mg/mL of either Silymarin or Nano-Silymarin, and compared to DMSO-treated and untreated (control) cells. **(B)** The relative mRNA expression of ERK was similarly assessed under the same treatment conditions. **(C and D)** The mRNA expression levels of P53 and CAS3 were also evaluated in Caco-2 cells following treatment with 1.25 mg/mL Silymarin or Nano-Silymarin, compared to DMSO-treated and control cells. Fold changes were calculated, and results are presented as mean ± SD from three independent experiments. Statistical significance was determined using a two-tailed Student's t-test on Ct values. A double asterisk (**) indicates a significant difference ($P < 0.01$).

Silymarin extract effectively blocks TNF-α signaling and activate IL-6, IL-4 and IL-10 production

To investigate the potential immunomodulatory effects of both Silymarin and Nano-Silymarin on treated cancer cells, the levels of several key cytokines were measured in Caco-2 cells following a 24-hour treatment with 1.25 mg/mL of either compound. Specifically, TNF-α, a marker of necrotic activity, IL-6, an important cytokine in innate immune signaling, and the anti-inflammatory cytokines IL-4 and IL-10 were assessed. Interestingly, treatment with original form of Silymarin alone resulted in a time-dependent increase in IL-6 levels in the culture medium, whereas Nano-Silymarin had only a minimal effect on IL-6 production (Figure 6A). In contrast, TNF-α levels significantly increased over time in cells treated with Nano-Silymarin, while Silymarin-treated cells exhibited a clear reduction in TNF-α expression (Figure 6B). Moreover, Silymarin treatment led to a substantial and time-dependent rise in IL-4 and IL-10 levels, a pattern not observed with Nano-Silymarin (Figures 6C and 6D). These findings suggest a dual role for Silymarin: it not only suppresses TNF-α signaling but also promotes IL-6 production, which may contribute to the initiation of PCD. Additionally, the elevated IL-4 and IL-10 levels point to the anti-inflammatory properties of Silymarin, implicating its influence on both necrotic activity and immune regulation in colon cancer cells.

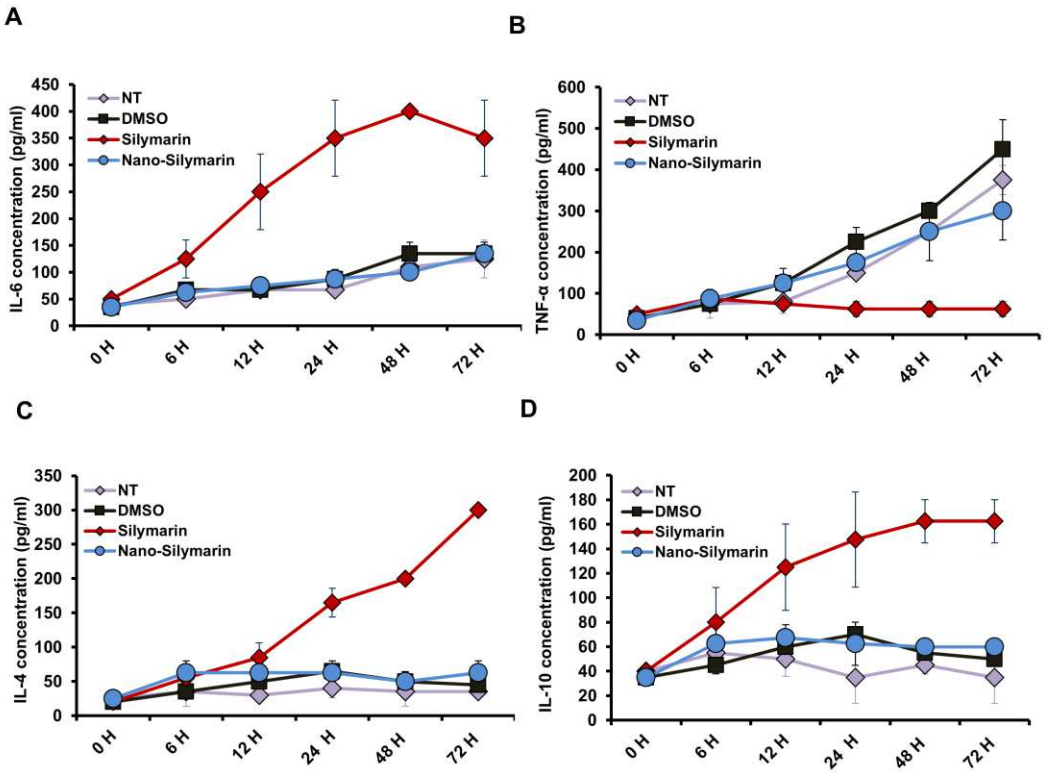


Figure 6: Quantification of IL-6 and TNF-α in treated Caco-2 cells

(A) TNF-α concentrations (pg/ml) measured over time in the culture media of Caco-2 cells pretreated with 5 µM Selenium or Nano-Selenium, compared to control-treated cells. (B) IL-6 concentrations (pg/ml) measured over time in the culture media of Caco-2 cells pretreated with 5 µM Selenium or Nano-Selenium, compared to control-treated cells. Error bars indicate SD from four replicates. Data represent results from three independent experiments.

Discussion

Silymarin, a flavonolignan complex extracted from *Silybum marianum* (milk thistle), is well-recognized for its antioxidant, hepatoprotective, and anti-inflammatory properties. However, its clinical effectiveness is limited due to poor water solubility and low bioavailability [25]. To address these limitations, nanotechnology has been employed to produce Nano-Silymarin, which enhances solubility, bioavailability, cellular uptake, and therapeutic efficacy. In this study, a nanomodified form of Silymarin was synthesized using Span 80 as a surfactant, facilitating nanoparticle size reduction under high pressure and encapsulation within lipid carriers. The primary objective was to evaluate the anticancer potential of both the original and nanomodified forms of Silymarin in colon cancer cells, while also considering their cytotoxicity toward normal colon epithelial cells. Surprisingly, the results revealed that the unmodified (original) form of Silymarin demonstrated superior ability to inhibit cancer cell proliferation compared to its nanomodified counterpart. This was evidenced by a more pronounced reduction in cell viability and cell survival, as well as increased LDH release following treatment. Furthermore, the original Silymarin formulation significantly suppressed TNF-α production in cancer cells, while upregulating IL-6, along with elevated levels of IL-4 and IL-10. This cytokine profile suggests that Silymarin may promote programmed cell death (PCD) and modulate the cellular immune response. In terms of gene expression, the original Silymarin was more effective in downregulating Raf-1 and ERK, key genes involved in cell proliferation, and simultaneously upregulating P53, a tumor suppressor gene. This led to activation of Caspase-3 (CAS3), a critical mediator in the apoptotic signaling pathway. Based on these findings, we hypothesize that the original form of Silymarin is more effective in inhibiting cancer cell proliferation than its nanomodified version.

While nanotechnology often aims to enhance pharmacological properties, it may sometimes lead to premature drug release, poor stability, or inefficient cellular uptake. In contrast, the unmodified form may allow sustained release and prolonged exposure of

cancer cells to active compounds, enhancing therapeutic effects [14]. Moreover, during the nanoparticle formulation process, key bioactive components such as silybin may undergo chemical modification, degradation, or reduced activity due to interactions with carriers or solvents [26]. This can compromise the overall anti-cancer efficacy. Some studies also report that inefficient nanoparticle internalization can limit drug delivery to intracellular targets [27,28]. Additionally, as Silymarin is a complex mixture of synergistic flavonolignans, nano-encapsulation might isolate or exclude certain constituents, disrupting this natural synergy and reducing therapeutic potential [29].

Notably, as potential target for Silymarin, the MAPK/ERK pathway, also referred to as the Ras-Raf-MEK-ERK pathway, is a sequence of proteins within a cell that relays signals from a receptor on the cell's surface to the DNA in the cell's nucleus [30]. The signaling process begins when a molecule binds to the receptor on the cell's surface and concludes with the DNA in the nucleus activating a protein that triggers changes in the cell, such as cell division and autophagic machinery [31]. This pathway includes several proteins, such as mitogen-activated protein kinases (MAPKs), originally known as extracellular signal-regulated kinases (ERKs), which communicate by adding phosphate groups to neighboring proteins, thereby acting as "on" or "off" switches [32]. When a protein in this pathway mutates, it can become locked in the "on" or "off" position, a key event in the development of many cancers. In fact, components of the MAPK/ERK pathway were initially discovered in cancer cells, and drugs that can reverse the "on" or "off" state are being explored as potential cancer treatments [33]. The ERK signaling pathway plays an essential role in cell growth, differentiation, and proliferation. It is involved in various processes, including phosphorylation and nucleocytoplasmic shuttling. Additionally, the epidermal growth factor receptor (EGFR), part of the ErbB family of receptor tyrosine kinases, is linked to cancer development and progression [34]. Cytokines like TNF-α also affect cancer cell proliferation, metastasis, and immune responses, and their regulation presents potential therapeutic opportunities for cancer treatment [35]. One the other hand, the tumor suppressor protein P53 plays a central role in regulating apoptosis, cell cycle arrest, and DNA repair by interacting with multiple

proteins. This process activates caspase-9, which, through cleavage, subsequently activates the executioner caspases-3 and -7 [36].

Our comprehensive study indicates that nanomodification of naturally occurring products may lead to unexpected outcomes when compared to their original forms. These differences may result from chemical modifications, degradation, or reduced activity of bioactive compounds during nanoprocessing. Additionally, inefficient internalization of nanoparticles can hinder effective drug delivery to intracellular targets. This was evident in our findings with Silymarin extract and its nanomodified form: the original extract demonstrated greater efficacy in regulating oncogene expression, promoting tumor suppressor gene P53 activation, which is crucial for apoptotic signaling and programmed cell death in cancer cells, and maintaining its biological roles as an anti-inflammatory and antioxidant agent.

Conclusion

Colorectal cancer, encompassing colon and rectal tumors, remains one of the most prevalent malignancies worldwide. In recent years, its epidemiological trends have shifted, with a rising incidence among younger populations and in regions experiencing dietary and lifestyle changes. Silymarin, a plant-derived extract recognized for its antioxidant, anti-inflammatory, and anticancer properties, has attracted growing attention as a potential therapeutic agent. This study aimed to develop a nanostructured formulation of Silymarin (Nano-Silymarin), evaluate its anticancer potential relative to the original extract, assess cytotoxicity, and explore the underlying molecular mechanisms in colon cancer cells. Nano-Silymarin was prepared by dissolving Silymarin in an oil phase containing Span 80 as an emulsifier, followed by high-pressure homogenization to produce droplets smaller than 100 nm. The antiproliferative effects of Nano-Silymarin were tested on Caco-2 colon cancer cells and compared with the native extract in both Caco-2 and NCM-460 normal colon epithelial cells. Findings showed that the original extract inhibited Caco-2 cell viability more effectively at lower concentrations than Nano-Silymarin, while exhibiting minimal toxicity toward normal epithelial cells. In contrast, Nano-Silymarin significantly reduced the viability of NCM-

460 cells at similar concentrations. At 1.25 mg/mL, the original Silymarin extract significantly decreased cancer cell viability and induced apoptosis in nearly 50% of Caco-2 cells, as measured by Annexin V flow cytometry, without compromising the viability of normal cells. qRT-PCR analysis revealed that the native extract downregulated Raf-1 and ERK, key components of the MAPK signaling pathway, while upregulating the tumor suppressor P53 and apoptotic marker CAS3. ELISA assays further indicated that, unlike the Nano-Silymarin formulation, the original extract induced a time-dependent reduction in TNF-α levels and an increase in IL-6, which promotes apoptotic signaling, alongside progressive elevations in anti-inflammatory cytokines IL-4 and IL-10. In conclusion, the original Silymarin extract demonstrated greater anticancer efficacy than its nanostructured counterpart by inhibiting proliferative pathways and promoting IL-6 and P53-mediated apoptosis, while maintaining a favorable safety profile in normal colon epithelial cells. Our study reveals that nanomodifying naturally occurring products can lead to unexpected outcomes due to chemical alterations, degradation, or reduced activity of bioactive compounds, as well as inefficient nanoparticle internalization. This was evident with Silymarin, where the original extract showed superior efficacy in regulating oncogene expression, activating the tumor suppressor gene P53 for apoptotic signaling, and retaining its anti-inflammatory and antioxidant functions.

Declarations

Ethics approval

Not applicable

Consent to participate

Not applicable

Consent to publish

Not applicable

Data availability statement

The datasets used and/or analyzed during the current study are available from the corresponding author on reasonable request.

Conflicting interests

All authors declare that there are no conflicts of interest.

Funding

Not applicable.

Authors' contributions

NF, MD, and AM, conducted experiments. KB, MA, AF, and AE assisted in supervising and conceptualizing the experiments. HK developed the research plan, led the overall study, analyzed and interpreted the results, and organized and wrote the manuscript.

Acknowledgements

Not applicable

References

1. Hossain MS, Karuniawati H, Jairoun AA, Urbi Z, Ooi DJ, John A, et al. Colorectal Cancer: A Review of Carcinogenesis, Global Epidemiology, Current Challenges, Risk Factors, Preventive and Treatment Strategies. Cancers. 2022. doi:10.3390/cancers14071732

2. Maher E, Gedawy G, Fathy W, Farouk S, El Maksoud AA, Guirgis AA, et al. Hsa-miR-21-mediated cell death and tumor metastases: A potential dual response during colorectal cancer development. Middle East J Cancer. 2020;11: 483–492. doi:10.30476/mejc.2020.83146.1139

3. Mohamed E-SA, Bassiouny K, Alshambky AA, Khalil H. Anticancer Properties of N,N-dibenzylasparagine as an Asparagine (Asp) analog, Using Colon Cancer Caco-2 Cell Line. Asian Pacific J Cancer Prev. 2022;23: 2531–2540. doi:10.31557/APJCP.2022.23.7.2531

4. Jones E, Duan Z, Nguyen TT, Giordano SH, Zhao H. Adjuvant 5-Fluorouracil/leucovorin, capecitabine, and oxaliplatin-related regimens for stage II/III colon cancer patients 66 years or older. Cancer Med. 2023;12: 2389–2406. doi:https://doi.org/10.1002/cam4.5078

5. Garrido Martínez MT, Rodríguez Jorge M, García Giménez I, Guzmán Ramos MI, Grutzmancher Sáiz S, Aviñó Tarazona V. Toxicity of the FOLFOX-6 regimen, with or without 5-fluorouracil bolus, in metastatic colorectal cancer. Farm Hosp. 2025;49: T154–T159. doi:10.1016/j.farma.2024.12.006

6. Surai PF. Silymarin as a Natural Antioxidant: An Overview of the Current Evidence and Perspectives. Antioxidants. 2015. pp. 204–247. doi:10.3390/antiox4010204

7. Aghemo A, Alekseeva OP, Angelico F, Bakulin IG, Bakulina N V, Bordin D, et al. Role of silymarin as antioxidant in clinical management of chronic liver diseases: a narrative review. Ann Med. 2022;54: 1548–1560.

doi:10.1080/07853890.2022.2069854

8. Fried MW, Navarro VJ, Afdhal N, Belle SH, Wahed AS, Hawke RL, et al. Effect of Silymarin (Milk Thistle) on Liver Disease in Patients With Chronic Hepatitis C Unsuccessfully Treated With Interferon Therapy: A Randomized Controlled Trial. JAMA. 2012;308: 274–282. doi:10.1001/jama.2012.8265

9. Jaffar HM, Al-Asmari F, Khan FA, Rahim MA, Zongo E. Silymarin: Unveiling its pharmacological spectrum and therapeutic potential in liver diseases—A comprehensive narrative review. Food Sci Nutr. 2024;12: 3097–3111. doi:https://doi.org/10.1002/fsn3.4010

10. Wang Y, Yuan A-J, Wu Y-J, Wu L-M, Zhang L. Silymarin in cancer therapy: Mechanisms of action, protective roles in chemotherapy-induced toxicity, and nanoformulations. J Funct Foods. 2023;100: 105384. doi:https://doi.org/10.1016/j.jff.2022.105384

11. Wang B, Hu S, Teng Y, Chen J, Wang H, Xu Y, et al. Current advance of nanotechnology in diagnosis and treatment for malignant tumors. Signal Transduct Target Ther. 2024;9: 200. doi:10.1038/s41392-024-01889-y

12. Anand U, Dey A, Chandel AKS, Sanyal R, Mishra A, Pandey DK, et al. Cancer chemotherapy and beyond: Current status, drug candidates, associated risks and progress in targeted therapeutics. Genes Dis. 2023;10: 1367–1401. doi:https://doi.org/10.1016/j.gendis.2022.02.007

13. Ioele G, Chieffallo M, Occhiuzzi MA, De Luca M, Garofalo A, Ragno G, et al. Anticancer Drugs: Recent Strategies to Improve Stability Profile, Pharmacokinetic and Pharmacodynamic Properties. Molecules. 2022. doi:10.3390/molecules27175436

14. Chehelgerdi M, Chehelgerdi M, Allela OQB, Pecho RDC, Jayasankar N, Rao DP, et al. Progressing nanotechnology to improve targeted cancer treatment: overcoming hurdles in its clinical implementation. Mol Cancer. 2023;22: 169.

doi:10.1186/s12943-023-01865-0

15. Manke A, Wang L, Rojanasakul Y. Mechanisms of Nanoparticle-Induced Oxidative Stress and Toxicity. Biomed Res Int. 2013;2013: 942916. doi:https://doi.org/10.1155/2013/942916

16. Elsayed I, El-Dahmy RM, Elshafeey AH, Abd El Gawad NA, El Gazayerly ON. Tripling the Bioavailability of Rosuvastatin Calcium Through Development and Optimization of an In-Situ Forming Nanovesicular System. Pharmaceutics. 2019. doi:10.3390/pharmaceutics11060275

17. Abdelsattar S, Al-Amodi HS, Kamel HF, Al-Eidan AA, Mahfouz MM, El khashab K, et al. Effective Targeting of Glutamine Synthetase with Amino Acid Analogs as a Novel Therapeutic Approach in Breast Cancer. International Journal of Molecular Sciences. 2025. doi:10.3390/ijms26010078

18. Dabous E, Alalem M, Awad AM, Elawdan KA, Tabl AM, Elsaka S, et al. Regulation of KLRC and Ceacam gene expression by miR-141 supports cell proliferation and metastasis in cervical cancer cells. BMC Cancer. 2024;24: 1091. doi:10.1186/s12885-024-12794-6

19. Guirgis SA, El-Halfawy KA, Alalem M, Khalil H. Legionellapneumophila induces methylomic changes in ten-eleven translocation to ensure bacterial reproduction in human lung epithelial cells. J Med Microbiol. 2023;72. doi:10.1099/jmm.0.001676

20. Shoaib H, Negm A, Abd El-Azim AO, Elawdan KA, Abd-ElRazik M, Refaai R, et al. Ameliorative effects of Turbinaria ornata extract on hepatocellular carcinoma induced by diethylnitrosamine in-vivo. J Mol Histol. 2024. doi:10.1007/s10735-024-10263-9

21. Awad AM, Dabous E, Alalem M, Alalem N, Nasr ME, Elawdan KA, et al. MicroRNA-141-regulated KLK10 and TNFSF-15 gene expression in hepatoblastoma cells as a novel mechanism in liver carcinogenesis. Sci Rep. 2024;14: 13492. doi:10.1038/s41598-024-63223-4

22. Alalem M, Dabous E, Awad AM, Alalem N, Guirgis AA, El-Masry S, et al. Influenza a virus regulates interferon signaling and its associated genes; MxA and STAT3 by cellular miR-141 to ensure viral replication. Virol J. 2023;20: 183. doi:10.1186/s12985-023-02146-4

23. Khalil H, Arfa M, El-Masrey S, EL-Sherbini S, Abd-Elaziz A. Single nucleotide polymorphisms of interleukins associated with hepatitis C virus infection in Egypt. J Infect Dev Ctries. 2017;11: 261–268. doi:10.3855/jidc.8127

24. Elawdan KA, Farouk S, Aref S, Shoaib H, El-Razik MA, Abbas NH, et al. Association of vitamin B12/ferritin deficiency in cancer patients with methylomic changes at promotors of TET methylcytosine dioxygenases. Biomark Med. 2022;16: 959–970. doi:10.2217/bmm-2022-0158

25. Polyak SJ, Morishima C, Lohmann V, Pal S, Lee DYW, Liu Y, et al. Identification of hepatoprotective flavonolignans from silymarin. Proc Natl Acad Sci. 2010;107: 5995–5999. doi:10.1073/pnas.0914009107

26. Bukke SPN, Venkatesh C, Bandenahalli Rajanna S, Saraswathi TS, Kusuma PK, Goruntla N, et al. Solid lipid nanocarriers for drug delivery: design innovations and characterization strategies—a comprehensive review. Discov Appl Sci. 2024;6: 279. doi:10.1007/s42452-024-05897-z

27. Zhang R, Qin X, Kong F, Chen P, Pan G. Improving cellular uptake of therapeutic entities through interaction with components of cell membrane. Drug Deliv. 2019;26: 328–342. doi:10.1080/10717544.2019.1582730

28. Barua S, Mitragotri S. Challenges associated with penetration of nanoparticles across cell and tissue barriers: A review of current status and future prospects. Nano Today. 2014;9: 223–243. doi:https://doi.org/10.1016/j.nantod.2014.04.008

29. Mastron JK, Siveen KS, Sethi G, Bishayee A. Silymarin and hepatocellular carcinoma: a systematic, comprehensive, and critical review. Anticancer Drugs. 2015;26. Available: https://journals.lww.com/anti-

cancerdrugs/fulltext/2015/06000/silymarin_and_hepatocellular_carcinoma__a.1.aspx

30. Bahar ME, Kim HJ, Kim DR. Targeting the RAS/RAF/MAPK pathway for cancer therapy: from mechanism to clinical studies. Signal Transduct Target Ther. 2023;8. doi:10.1038/s41392-023-01705-z

31. Khalil H, Elhady AA, Elawdan KA, Mohamed D, Mohamed D, Abd AI, et al. The Mechanical Autophagy as a Part of Cellular Immunity ; Facts and Features in Treating the Medical Disorders The Mechanical Autophagy as a Part of Cellular Immunity ; Facts and Features in Treating the Medical Disorders. Immunol Invest. 2020;00: 1–24. doi:doi.org/10.1080/08820139.2020.1828453

32. El-Fadl HMA, Hagag NM, El-Shafei RA, Khayri MH, El-Gedawy G, Maksoud AIA El, et al. Effective Targeting of Raf-1 and Its Associated Autophagy by Novel Extracted Peptide for Treating Breast Cancer Cells. Front Oncol. 2021;11: 3317. doi:10.3389/fonc.2021.682596

33. Liu F, Yang X, Geng M, Huang M. Targeting ERK, an Achilles' Heel of the MAPK pathway, in cancer therapy. Acta Pharm Sin B. 2018;8: 552–562. doi:https://doi.org/10.1016/j.apsb.2018.01.008

34. Grandal MV, Madshus IH. Epidermal growth factor receptor and cancer: control of oncogenic signalling by endocytosis. J Cell Mol Med. 2008;12: 1527–1534. doi:https://doi.org/10.1111/j.1582-4934.2008.00298.x

35. Conlon KC, Miljkovic MD, Waldmann TA. Cytokines in the Treatment of Cancer. J Interf Cytokine Res. 2018;39: 6–21. doi:10.1089/jir.2018.0019

36. Sheridan C, Delivani P, Cullen SP, Martin SJ. Bax- or Bak-Induced Mitochondrial Fission Can Be Uncoupled from Cytochrome c Release. Mol Cell. 2008;31: 570–585. doi:10.1016/j.molcel.2008.08.002